Turbulent Combustion of Spherical Fuel-Rich Hydrogen Pockets

J. B. Bell[a], M. S. Day[a,c], J. F. Grcar[b] and A. E. Lutz[b]
[a] Lawrence Berkeley National Laboratory, Berkeley, CA
[b] Sandia National Laboratories, Livermore, CA
[c] Corresponding author: MSDay@lbl.gov

Recent experimental investigations of combustion in diesel engines showed that the initial premix burn creates pockets of soot and fuel that must burn out in a diffusion-flame mode in order to complete the combustion [5, 6]. Understanding the final stages of this process is critical to predicting the emissions of soot and NO_x.

This effort uses numerical simulations to investigate burnout of diffusion flames that result from the autoignition of rich premixtures created by the injection process. An initial model is developed using hydrogen gas as a combustion fuel. A three-dimensional diffusion flame is established around an initially spherical fuel pocket that is formed when a rich (equivalence ratio of 4) mixture of hydrogen and air ignites. After the premixed ignition, the remaining fuel mixes with the surrounding air by molecular diffusion and turbulent mixing, forming a wrinkled diffusion flame. The numerical method uses a dynamically adaptive mesh to resolve the flame and turbulent flow field. A detailed reaction mechanism for the hydrogen chemical kinetics and heat release (9 species, 27 reactions) is employed based on the relevant components of the GRI-1.2 [7] mechanism for methane combustion.

Mathematical Model

The computational methodology incorporated for this work is a generalization to three dimensions of that presented in Day and Bell [4]. The model is based on a conservative form of the low Mach number combustion model introduced by Rehm and Baum [11], subsequently derived from low Mach number asymptotic analysis by Majda and Sethian [9]. We consider a gaseous mixture, ignoring Soret and Dufour effects, body forces and radiative heat transfer, and assume a mixture model for species diffusion [8, 13]. For an unconfined domain, we have

$$\frac{\partial \rho U}{\partial t} + \nabla \cdot \rho UU = -\nabla \pi + \nabla \cdot \tau, \tag{1}$$

$$\frac{\partial \rho Y_m}{\partial t} + \nabla \cdot U \rho Y_m = \nabla \cdot \rho \mathcal{D}_m \nabla Y_m + \dot{\omega}_m, \tag{2}$$

$$\frac{\partial \rho h}{\partial t} + \nabla \cdot U \rho h = \nabla \cdot \lambda \nabla T + \sum_m \nabla \cdot \rho h_m(T) \mathcal{D}_m \nabla Y_m \tag{3}$$

where ρ is the density, U is the velocity, π is the pressure variation from a uniform ambient pressure, Y_m is the mass fraction of species m, h is the mass-weighted enthalpy of the gas mixture, T is the temperature, and $\dot{\omega}_m$ is the net production rate for species m due to chemical reactions. Also, λ is the thermal conductivity, τ is the stress tensor, $c_{p,mix}$ is the specific heat of the mixture and $h_m(T)$ and $\mathcal{D}_m$ are the enthalpy and species mixture-averaged diffusion coefficients of species m, respectively. These evolution equations are supplemented by an equation of state for a perfect gas mixture:

$$p_0 = \rho R_{mix} T = \rho \mathcal{R} T \sum_m \frac{Y_m}{W_m} \tag{4}$$

where W_m is the molecular weight of species m.

In the low Mach number limit, the thermodynamic pressure given by equation (4) remains approximately constant as the flow evolves. Differentiating the equation of state in the frame of the fluid, and using the conservation equations to replace advective derivatives, we obtain a constraint on the evolving velocity field:

$$\nabla \cdot U = \frac{1}{\rho c_p T}\left(\nabla \cdot \lambda \nabla T + \sum_m \rho \mathcal{D}_m \nabla Y_m \cdot \nabla h_m\right) + \tag{5}$$
$$+ \frac{1}{\rho}\sum_m \frac{W}{W_m}\nabla \cdot \rho \mathcal{D}_m \nabla Y_m \; - \frac{1}{\rho}\sum_m \left(\frac{h_m(T)}{c_{p,mix}T} - \frac{W}{W_m}\right)\dot{\omega}_m \equiv S$$

where $W = (\sum_m Y_m/W_m)^{-1}$ and $c_{p,mix} = \sum_m Y_m dh_m/dT$.

Numerical methodology

Our computational approach uses a hierarchical adaptive mesh refinement (AMR) algorithm based on an approximate projection formulation for integrating the momentum equations developed by Almgren *et al.* [1], and subsequently extended to low Mach number reacting flows by Pember *et al.* [10]. The projection algorithm is coupled to conservation equations for chemical species and enthalpy. The single-grid algorithm is implemented in a structured uniform grid setting, and incorporated into an AMR framework that employs a recursive time-stepping procedure over refinement levels. We sketch the numerical implementation below; the reader is referred to Day and Bell [4] for details.

The single-grid scheme is a fractional step algorithm that first advances momentum, species and enthalpy equations with a lagged perturbational pressure. We discretize equations (1–3) using a second-order Godunov scheme for the convective terms and a time-centered Crank-Nicolson discretization for diffusion. The Godunov discretization incorporates in intermediate projection so that the velocity field used to compute the advective derivatives satisfies the constraint (5). Because the transport coefficients depend on both temperature and composition, we adopt a sequential, predictor-corrector scheme to guarantee second-order treatment of nonlinear diffusion effects. The chemistry is advanced using time-implicit backward differentiation methods in VODE [2]. The advection/diffusion and chemistry components of the algorithm are time-split symmetrically to ensure that the composite algorithm remains second-order.

The velocity field resulting from the advection/diffusion/chemistry step is then projected using a density-weighted approximate projection to enforce the velocity divergence constraint (5). Numerically, the projection step requires the solution of a variable-coefficient linear elliptic equation. In addition to enforcing the divergence constraint, the projection also determines an update to the perturbational pressure. The explicit procedure for the treatment of advection terms necessitates a CFL-type time-step restriction. Since the advective time scale is typically larger than the fastest time scales associated with the chemical kinetics, this does not appear to be a serious disadvantage for time-dependent simulations.

The extension of the above algorithm to adaptive mesh refinement is based on a hierarchical refinement strategy. Our methodology uses a system of overlaid grids with successively finer spacing in time and space. Fine grids are formed by uniformly dividing coarse cells in each direction. Increasingly finer levels, each consisting of a union of rectangular grid patches, overlay underresolved portions of the coarser grid levels until the solution is adequately resolved. An error estimation procedure identifies where refinement is needed and grid generation procedures dynamically create or remove rectangular fine grid patches as the solution is evolved and requirements change.

The complete adaptive algorithm has a number of desirable properties. The overall method is second-order accurate in space and time, and discretely conserves species mass and enthalpy. Furthermore, the algorithm satisfies a free-stream preservation property so that nonreacting isothermal flow remains numerically isothermal during species transport.

The methodology has been implemented for distributed memory parallel processors using the BoxLib class libraries described by Rendleman *et al.* [12]. In this approach, grid patches are distributed to processors using a heuristic knapsack algorithm to balance the computational work (see Crutchfield [3]). For nonreacting fluid flows, work estimates based on the number of cells in a grid provide an effective load balancing strategy.

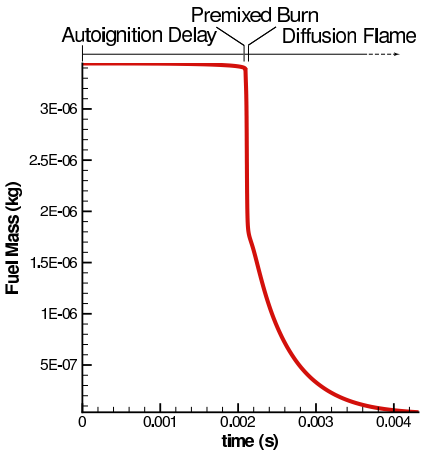

Figure 1. History of integrated H_2 fuel mass during evolution of the system. After a delay, the fuel-rich mixture goes through a rapid premixed burn until the O_2 is depleted from the fuel sphere. Nonpremixed combustion then consumes the remaining fuel on a comparatively longer timescale.

However, for reacting flows there can be considerable variability in the time required to integrate the kinetics equations depending on temperature and composition. To account for this variability we monitor the number of rate evaluations required to integrate the kinetics equations and use the data to estimate the work required to advance the chemistry for each grid patch. These estimates are used for a separate, finer-grained load balancing step for the chemistry.

Results

The simulations reported here are a first attempt to study the burn-out of hot, rich pockets of fuel immersed in turbulent, high-pressure air. Initial temperature and pressure are uniform at 1000 K and 50 atm. These conditions correspond to those near top-dead-center in a typical diesel engine at the point when fuel is injected. A 1 cm diameter sphere of hydrogen and air mixed at equivalence ratio of four is placed at the center of a cubic three-dimensional domain 10 cm on a side. The equivalence ratio of the fuel region reflects the expected degree of mixing at the point when ignition occurs. A turbulent velocity field is initialized with the following energy spectrum

$$E(k) = C * (k^4/{k_o}^5) exp(-2 * (k/k_o)^2)$$

where k_o is the peak frequency ($12 cm^{-1}$ here). C is a constant used to specify the turbulent intensity; away from the fuel sphere, $C \rightarrow 0$ so that all boundaries of the system remain outflowing. The system is evolved in time though the complete consumption of hydrogen fuel.

The overall progress of the reaction is shown in Figure 1. The integrated fuel mass reveals three clearly defined phases of reaction. The first is the ignition delay period which can be predicted by 0-dimensional kinetic simulations. The second is the rapid consumption of fuel during the premixed combustion of the kernel. When the oxygen in the kernel is consumed, there is a marked slowing in the fuel consumption rate. This indicates a transition to non-premixed combustion. The progress of the nonpremixed combustion decreases as the local peaks in fuel concentration decline, thereby lessening their gradients. Understanding the final stages of burn-out is critical to explaining the emissions of soot and nitric oxides from diesel engines.

Figure 2 depicts volume renderings of the temperature profile near the hydrogen flame kernal at 2.1 and 2.4 ms. Each image is accompanied by a slice plane taken through the center of the data and colored according to the thermal scale shown. Figure 2(a) depicts the temperature field just after the period of premixed combustion within the flame kernel. The surface of the flame ball is wrinkled primarily from the turbulence imposed in the initial velocity field. Figure 2(b) depicts the temperature later in time, when

continued reactions occur in diffusion flames both at the periphery and, as will be seen, in the interior of the fuel-rich region. Preliminary evidence suggests that the marked increase in flame wrinkling at later stages result from a Rayleigh-Taylor instability, generated during the expansion of the hot, low-density core into the cooler, higher-density surroundings. In the slice planes of Figure 2(a), the surface of maximum temperature is seen to be a wrinkled but nearly spherical narrow region at the boundary of the fuel kernal. The maximum temperature occurs at the diffusion flame sheet, which is the point where the fuel and air mixture is stoichiometric. The temperature in the core is established by the rich premixed combustion phase, and so is lower than the peak temperature of the diffusion flame. In contrast, the late-time structure, Figure 2(b), shows that turbulent mixing has distributed regions of flame into the core of the original fuel-rich zone. In further investigation into the details of the flame structure we will examine the local mixture fraction to characterize the reaction in terms of diffusion flamelets and distributed reaction zones.

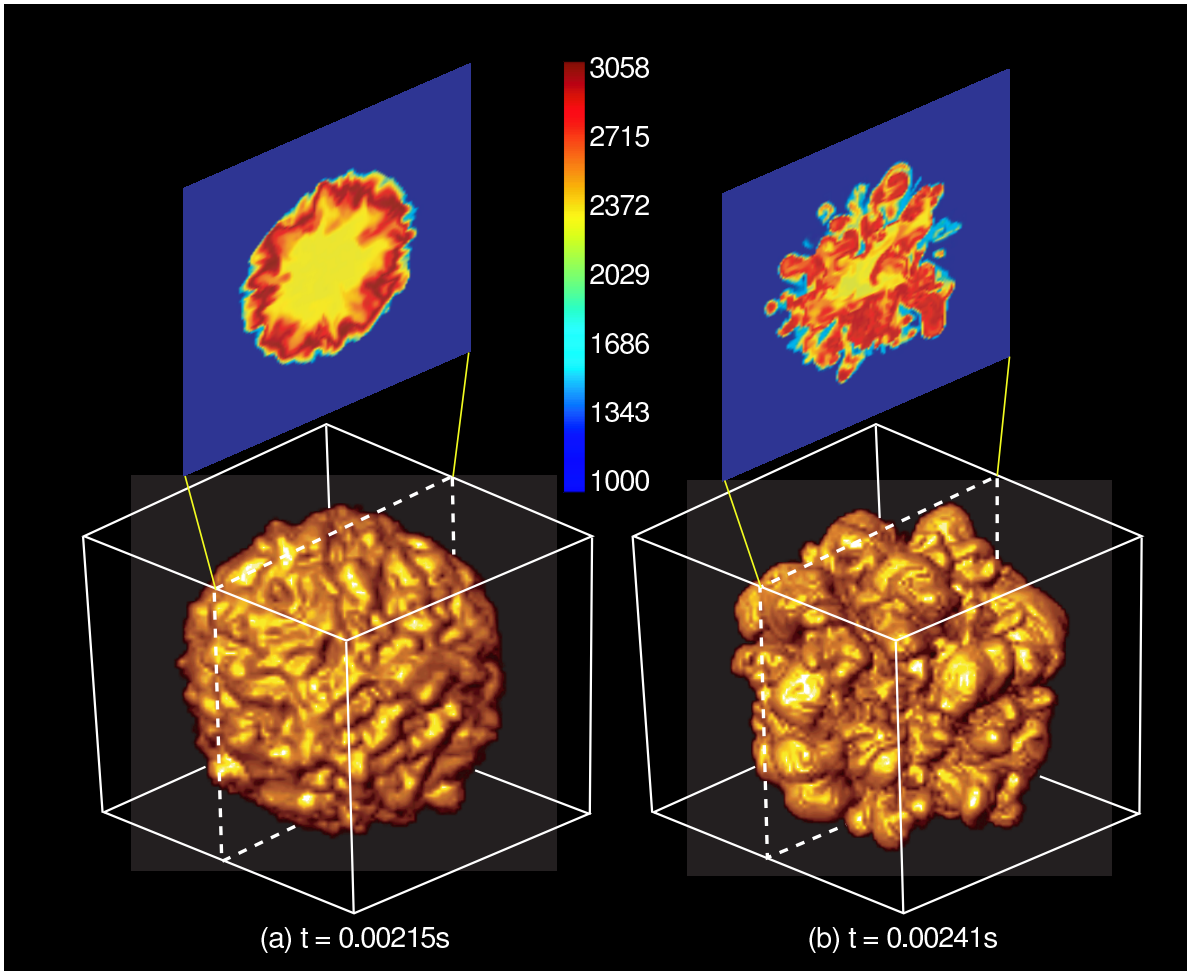

Figure 2. The temperature profiles near the flame kernal at (a) 2.1 ms and (b) 2.4 ms. The early-time image is just after the premixed burn, while the late-time image is well into the nonpremixed combustion. At the latter time, regions of the flame have been distributed into the core of the fuel-rich zone. Temperature is specified in K.

[1] A. S. Almgren, J. B. Bell, P. Colella, L. H. Howell, and M. Welcome. A conservative adaptive projection method for the variable density incompressible Navier-Stokes equations. *J. Comput. Phys.*, 142:1–46, 1998.

[2] P. N. Brown, G. D. Byrne, and A. C. Hindmarsh. VODE: A variable coefficient ode solver. *SIAM J. Sci. Stat. Comput.*, 10:1038–1051, 1989.

[3] W. Y. Crutchfield. Load balancing of an irregular algorithm. LLNL Report UCRL-JC-107679, LLNL, July 1991.

[4] M. S. Day and J. B. Bell. Numerical simulation of laminar reacting flows with complex chemistry. *Combust. Theory Model*, 4:535–556, 1999.

[5] J. E. Dec. *SAE*, 106:1319–1348, 1981.

[6] R. F. Flynn, R. P. Durrett, G. L. Hunter, A. O. zur Luye, O. C. Akinyemi, J. E. Dec, and C. K. Westbrook. SAE paper 990509, SAE, 1999.

[7] M. Frenklach, H. Wang, M. Goldenberg, G. P. Smith, D. M. Golden, C. T. Bowman, R. K. Hanson, W. C. Gardiner, and V. Lissianski. GRI-Mech—An optimized detailed chemical reaction mechanism for methane combustion. Gas Research Institute Report GRI-95/0058, Gas Research Institute, 1995. See also `http://www.me.berkeley.edu/gri_mech/`.

[8] R. J. Kee, G. Dixon-Lewis, J. Warnatz, M. E. Coltrin, and J. A. Miller. A FORTRAN computer code package for the evaluation of gas-phase multicomponent transport properties. Sandia National Laboratories Report SAND86-8246, Sandia National Laboratories, Livermore, 1986.

[9] A. Majda and J. A. Sethian. The derivation and numerical solution of the equations for zero Mach number combustion. *Combust. Sci. Tech.*, 42:185–205, 1985.

[10] R. B. Pember, L. H. Howell, J. B. Bell, P. Colella, W. Y. Crutchfield, W. A. Fiveland, and J. P. Jessee. An adaptive projection method for unsteady, low-Mach number combustion. *Comb. Sci. Tech.*, 140:123–168, 1998.

[11] R.G. Rehm and H.R. Baum. The equations of motion for thermally driven buoyant flows. *N.B.S.J.Res.*, 83:297–308, 1978.

[12] C. A. Rendleman, V. E. Beckner, M. Lijewski, W. Y. Crutchfield, and J. B. Bell. Parallelization of structured, hierarchical adaptive mesh refinement algorithms. *Computing and Visualization in Science*, 2000. Appears also as Lawrence Berkeley National Lab Report LBNL-43154.

[13] J. Warnatz. Influence of transport models and boundary conditions on flame structure. In N. Peters and J. Warnatz, editors, *Numerical methods in flame propagation*. Friedr. Viewweg and Sohn, Wiesbaden, 1982.